Acta Metallurgica, Vol. 28, pp. 621 to 632

0001-6160/80/0501-0621$02.00/0

INTERPHASE INTERFACES OF Au–Ag AND Au–Pd

M. HWANG, D. E. LAUGHLIN and I. M. BERNSTEIN

Department of Metallurgy and Materials Science, and The Center for the Joining of Materials, Carnegie-Mellon University, Pittsburgh, Pennsylvania 15213, U.S.A.

(*Received* 11 *September* 1979; *in revised form* 8 *October* 1979)

Abstract—The interfacial microstructure of {001} twist interphase boundaries in Au–Ag and Au–Pd bicrystal thin film couples has been investigated by transmission electron microscopy. The bicrystal thin film couples were produced by a new technique described herein. Examination of the bicrystal films showed that orthogonal grids of interphase boundary dislocations of ⟨110⟩ type formed in the {001} low-angle twist interphase boundaries of both Au–Ag and Au–Pd systems. The interfacial dislocations of Au–Ag interphase boundaries are similar to those of Au–Au, i.e., almost screw in character. In Au–Pd interphase boundaries, the interfacial dislocations show the mixed edge and screw character as expected.

The high-angle {001} twist interphase boundaries of Au–Ag and Au–Pd were also studied. The concidence lattice concept was applied to study the high-angle twist interphase boundaries. Several critical angles were obtained for both Au–Ag and Au–Pd systems. Orthogonal grids of secondary dislocations were observed in the {001} twist interphase boundary of Au–Ag thin film couples with the twist angle near 36.9°, the critical angle corresponding to the coincidence of $\Sigma = 5$. Experimental evidence of the interfacial dislocation structure of the high-angle twist interphase boundaries of Au–Pd has not yet been obtained. However, diffraction patterns do show the coincidence character in agreement with what was predicted.

Résumé—Nous avons étudié par microscopie électronique en transmission les joints interphases de torsion {001} dans des lames minces bicristallines de Au–Ag et Au–Pd. Les lames minces bicristallines étaient fabriquées par une technique nouvelle que nous décrivons. L'étude de ces films bicristallines a permis de mettre en évidence la formation de réseaux orthogonaux de dislocations ⟨110⟩ sur les sous-joints interphases de torsion {100} dans les deux systèmes Au–Ag et Au–Pd. Les dislocations des joints interphases du système Au–Ag ressemblent à celles du système Au–Au, c'est à dire qu'elles sont essentiellement vis. Dans les joints interphases du système Au–Pd, les dislocations présentaient un caractère mixte, comme on s'y attendait.

Nous avons également étudié dans les systèmes Au–Ag et Au–Pd les joints interphases {001} de grand angle de torsion. Nous avons appliqué le concept du réseau de coïncidence à l'étude des joints interphases de grand angle de torsion. Nous avons obtenu plusieurs angles critiques dans les deux systèmes. Nous avons observé des réseaux orthogonaux de dislocations secondaires dans des joints interphases {100} de torsion dans des couples Au–Ag en films minces, avec un angle de torsion proche de 36,9°, qui est l'angle critique correspondant à une coïncidence $\Sigma = 5$. Nous n'avons toutefois pas encore obtenu expérimentalement de structure de dislocations d'interfaces dans les joints interphases de grand angle de torsion du système Au–Pd. Cependant, les diagrammes de diffraction présentent de caractère de coïncidence, en accord avec nos prévisions.

Zusammenfassung—Die Grenzflächenmikrostruktur von {001} Drehungsinterphasengrenzen in Au–Ag und Au–Pd-bikristall-dünnen Filmpaaren wurde mit Hilfe der Durchstrahlungselektronenmikroskopie ermittelt. Die bikristall-dünnen Filmpaare wurden mit einer neuen Technik hergestellt, welche in dieser Arbeit beschrieben wird. Untersuchungen der Bikristallfilme zeigten, dass sich rechtwinklige Gitter von Interphasengrenzenversetzungen des ⟨110⟩ Types in den {001} Flachwinkel-Drehungsinterphasengrenzen des Au–Ag- sowohl wie auch des Au–Pd-Systems formten. Die Grenzflächenversetzungen der Au–Ag-Interphasengrenzen sind ähnlich zu denen der Au–Au, d.h. beinahe schraubenartig im Charakter. Wie erwartet wurde, zeigen die Grenzflächenversetzungen in Au–Pd-Interphasengrenzen die vermischte Kante und den schraubenartigen Charakter.

Auch die {001} Steilwinkel-Drehungsinterphasengrenzen von Au–Ag und Au–Pd wurden studiert. Der Begriff von übereinstimmenden Gittern wurde angewendet. Für beide Systeme wurden kritische Winkel gefunden. Rechtwinklige Gitter von sekundären Versetzungen erhielt man in der {001} Drehungsinterphasengrenze von Au–Ag-dünnen Filmpaaren mit dem Drehungswinkel nahe bei 36,9°, der kritische Winkel gemäss der Übereinstimmung von $\Sigma = 5$. Experimentelle Ergebrisse der Struktur der Grenzflächenversetzung von Steilwinkel- Drehungsinterphasengrenzen von Au–Pd konnten leider noch nicht erlangt werden. Wie dem auch sei, Beugungsdiagramme zeigen den übereinstimmenden Charakter, wie vorhergesagt wurde.

INTRODUCTION

Experimental studies have shown that in interfaces formed between epitaxial thin films of dissimilar metals of sufficiently small misfit and overgrowth thickness, mismatch will be accommodated entirely by homogeneous elastic strain in the film as long as the dissimilar metals have the same atomic configuration in their respective interfacial planes. As the thickness of an initially coherent film increases, however, the film becomes unstable and lattice spacing misfit dislocations are introduced at the interface with

a partial loss of coherency. These systems have been extensively studied [1–3] and have yielded important information on the structure and structural stability of these 'special' interfaces.

Balluffi and his coworkers [4–8] have extended these studies to the case of the interfacial structure in arbitrarily oriented twist misfit boundaries formed by mechanical joining of two gold single crystals. These now classical experiments have given a much clearer picture of the dislocation structure of low-angle twist boundaries, as well as the interfacial structure near higher angle coincidence boundaries, where it was shown that small deviation from perfect coincidence is accommodated by a network of screw dislocations.

We wish to report in this paper, the next step in such studies; namely, the structural behavior of *twist* interphase boundaries formed between single crystals of *dissimilar* metals. The production of low-angle and high-angle twist boundaries will be described for two cases, Au–Ag and Au–Pd. Since we believe the developed procedure to be original in nature, it will be described in some detail.

The Au–Ag couple represents the case of a very small difference in lattice parameter ($\sim 0.2\%$), while for Au–Pd it is much larger ($\sim 4.8\%$). In effect, the former should have a twist boundary structure very similar to, for example, Au–Au, while in the latter the structure should be readily observed to have mixed edge and screw character.

The geometry of this general case of the twist boundary between two dissimilar metallic thin films but with the same Bravais lattice has been theoretically investigated by Jesser and Kuhlmann-Wilsdorf, [9] in terms of a dislocation model. In their model a {001} twist interphase boundary of the cubic lattice contains an orthogonal dislocation grid. These dislocations have mixed edge and screw character to accommodate both the difference in lattice parameter and misorientation. The angle σ between the axis of the interfacial dislocations and their respective Burgers vectors is given by:

$$\sigma = \frac{\pi}{2} - \frac{\Delta\theta}{2} - \arctan\left(\frac{b_1 \sin(\Delta\theta)}{b_2 - b_1 \cos(\Delta\theta)}\right) \quad (1)$$

and the dislocation spacing,

$$S_D = \frac{b_1 b_2}{(b_1^2 + b_2^2 - 2b_1 b_2 \cos(\Delta\theta))^{1/2}} \quad (2)$$

where $\Delta\theta$ is the twist angle, b_1 and b_2 are the lattice constants of crystal 1 and crystal 2 in the 2-dimension interfacial reference lattices.

In the case of the {001} twist interface in the face-centered cubic Bravais lattice, b_1 and b_2 are the lattice parameters divided by $\sqrt{2}$, since the {001} plane of the fcc crystal forms a 2-D square lattice with a lattice constant equal to $a/\sqrt{2}$.

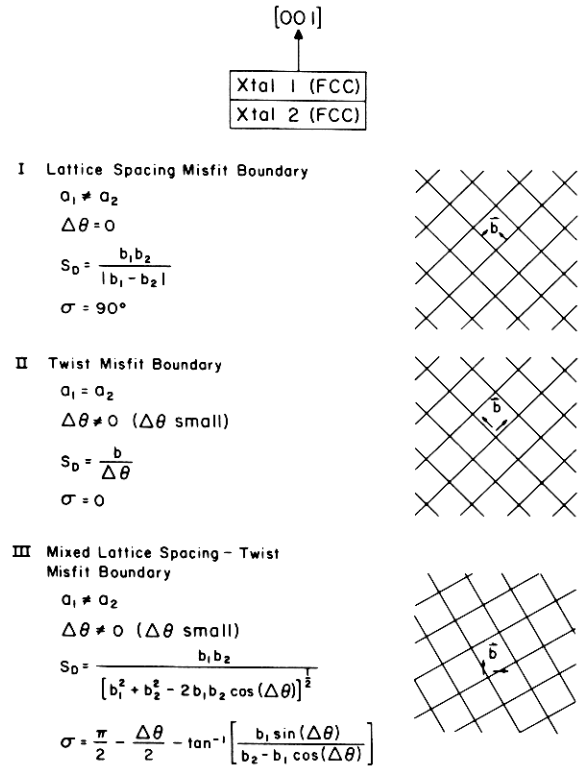

Fig. 1. Schematic representations of three special types of interfacial dislocation structures. a_1 and a_2 are the lattice parameters and b_1 and b_2 are the magnitude of Burgers vectors of corresponding crystals, $\Delta\theta$ is the twist angle about the common [001] axis of both crystals. S_D is the spacing of dislocation array and σ is the angle between the dislocation line and the corresponding Burgers vector.

Schematic representations of the lattice spacing misfit boundary, twist misfit boundary and mixed misfit boundaries in terms of their dislocation structure are shown in Fig. 1.

EXPERIMENTAL PROCEDURE

The dissimilar bi-metallic thin film couples studied in this investigation are gold–silver and gold–palladium. A single crystal epitaxial gold film about 400 Å thick, with its surface parallel to {001}, was vapor deposited onto a {001} cleavage face of a rocksalt (NaCl) substrate, on which an epitaxial layer of silver about 2000 Å thick had previously been deposited. The use of a pre-deposited silver film reduces the misfit between the gold film and the substrate and greatly improves the quality of the gold films. The {001} single crystal thin films of silver and palladium were about 800 Å and 500 Å thick, respectively. These were directly vapor deposited onto the {001} cleavage faces of rocksalt. This procedure was followed because we could not use the double-layer process due to the fact that we do not know of a pre-deposited material which can both provide a smaller misfit than that of the original substrate and be easily removed from the Ag or Pd.

The gold–silver and the gold–palladium bi-crystal couples were produced by the following procedures:

1. Metallic thin films still on their rocksalt substrates were cut into small pieces with edge dimensions about 1 mm × 1 mm. Since the edges followed the cleavage of rocksalt, these were parallel to ⟨100⟩ directions.
2. For silver and palladium films, the rocksalt substrates were then dissolved in the water and the floating films were placed on the tungsten grids. See Fig. 2, step 1.
3. For gold films, the rocksalt substrates and silver layers were dissolved away from the gold films by successive immersions in water and nitric acid. See Fig. 2, step 2.
4. The gold films were then placed on those tungsten grids to which the silver or palladium thin films had previously been placed. The approximate twist angle could easily be estimated from the angle between the edges of two films. See Fig. 2, step 3.

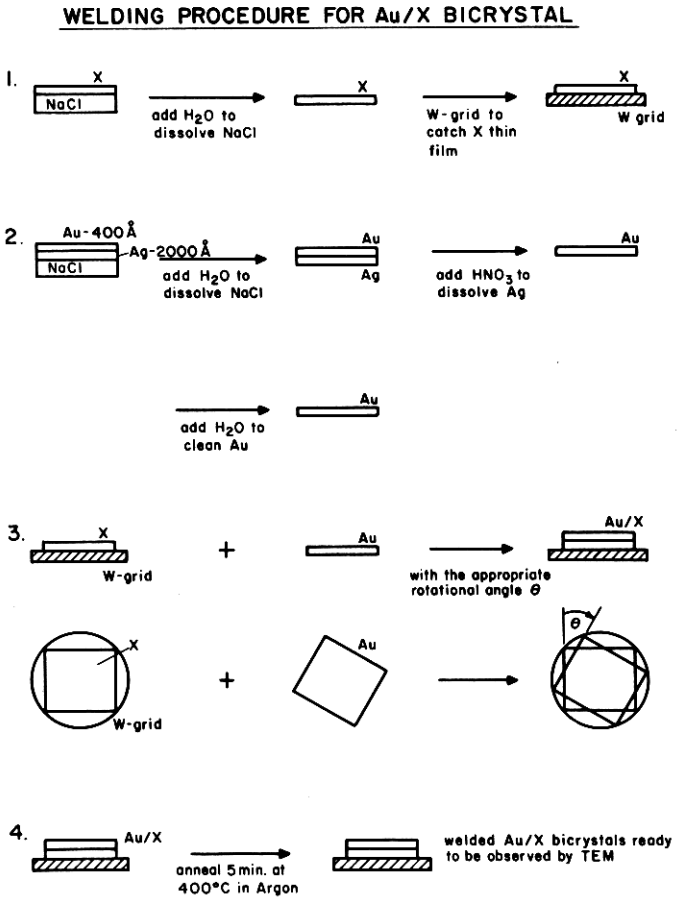

Fig. 2. Welding procedure for Au–X bicrystal thin film couples. X is either Ag or Pd. In step 3, the first line is the side view and the second line is the top view. The annealing condition shown in step 4 is a condition for Au–Ag couples. The appropriate annealing condition is dependent on the material and the twist angle.

5. After any necessary annealing treatment, the interfacial microstructures were examined by transmission electron microscopy on a JEOL 100B microscope, equiped with a double tilt stage, capable of $\pm 36°$ on one axis and $\pm 60°$ on a perpendicular axis.

It should be noted that no external pressure was used, and no pre-heat treatment was required. This allows us to investigate the earliest stages of dislocation formation.

EXPERIMENTAL RESULTS

Low angle {001} twist interphase boundaries for both Au–Ag and Au–Pd were examined in annealed bicrystal films. Two sets of orthogonal interfacial dislocations were observed for the two-beam diffraction condition, $\mathbf{g} = (200)$. Typical examples of such an interfacial dislocation network for Au–Ag and Au–Pd are shown in Figs. 3a and 4.

One set of dislocations is out of contrast when the $\mathbf{g} \cdot \mathbf{b} = 0$ criterion for zero contrast is met with a diffracting vector of $\mathbf{g} = (\bar{2}20)$, as shown in Fig. 3b. This implies that the Burgers vector is of the $\langle 110 \rangle$ type. The unique orientation of the dislocation axis was determined by comparing the bright field micrograph with the indexed diffraction pattern which had been

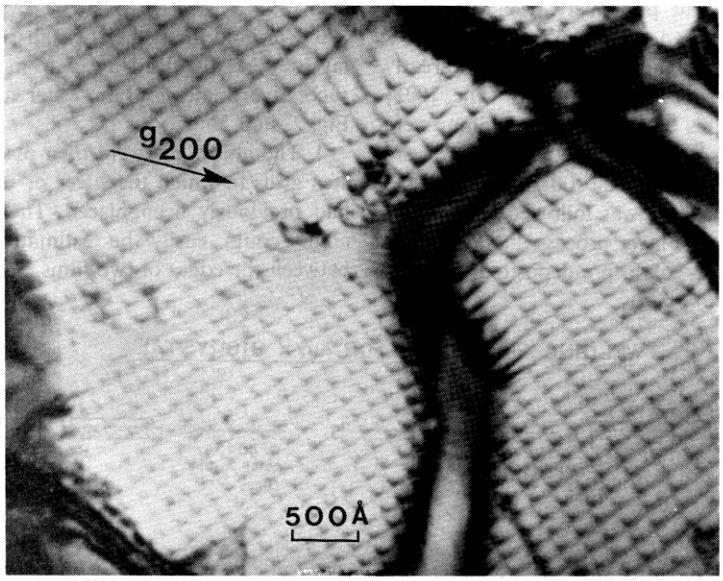

(a)

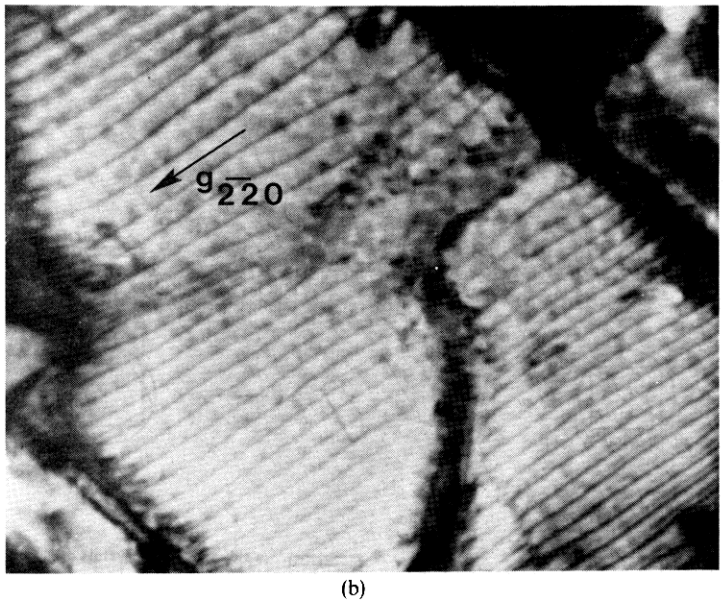

(b)

Fig. 3. (a) A cross grid dislocation network in the (001) interphase boundary of Au–Ag bimetallic thin film couple. Two mutually orthogonal sets are in contrast with $\mathbf{g} = (200)$. (b) Only one set of parallel dislocations appear when $\mathbf{g} = (\bar{2}20)$. Since the dislocation lines are almost parallel to the corresponding Burgers vectors, the dislocations are screw in character.

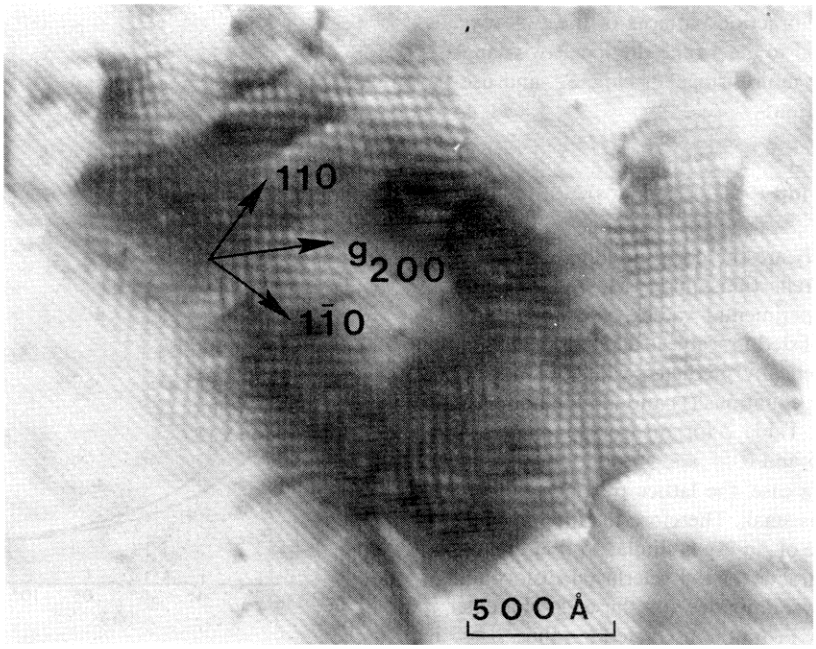

(a)

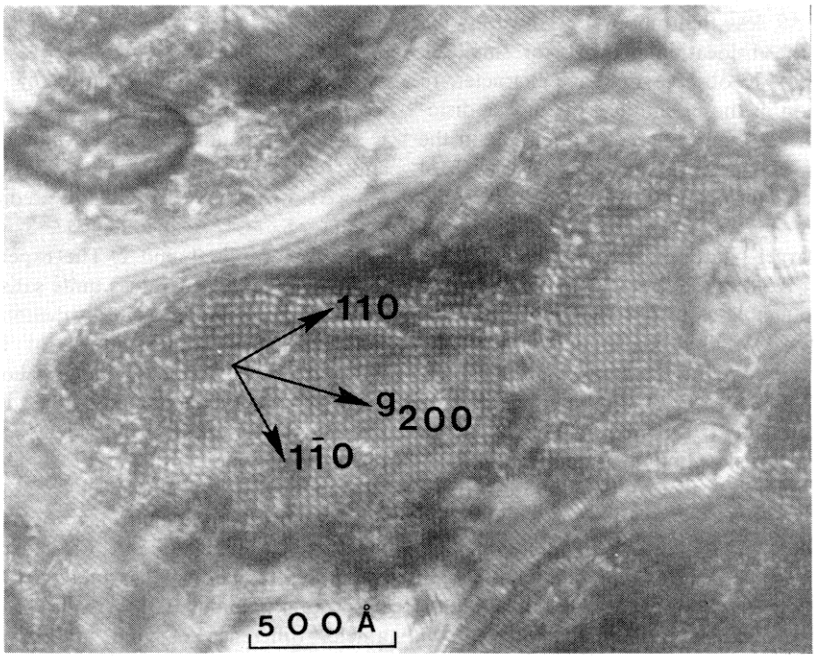

(b)

Fig. 4. Interphase boundary dislocation networks in (001) twist interfaces of Au–Pd. The dislocation lines are neither parallel nor perpendicular to ⟨110⟩, orientation of Burgers vectors. (a) The twist angle, $\Delta\theta$, is about 2.2°. The dislocation spacing, S_D, is 47 Å and σ is approx. 52°. (b) The twist angle, $\Delta\theta$, is about 4.5°. The dislocation spacing, S_D, is 31 Å and σ is approx. 29°.

rotated by the appropriate angle. From this information, the angle σ between the Burgers vector and the dislocation axis was obtained. The spacing of the interfacial dislocations, S_D, of a uniformly distributed dislocation array, was measured directly from the bright-field image.

The local twist angle was measured from the relative rotation between the simultaneously recorded

single crystal diffraction patterns of the two crystals. Another method to determine the local twist angle is to measure the moiré fringe spacing, S_m, and use the following equation:

$$S_m = \frac{d_1 d_2}{(d_1^2 + d_2^2 - 2d_1 d_2 \cos(\Delta\theta))^{1/2}} \quad (3)$$

where d_1 and d_2 are the corresponding d-spacings of the operating reflections in crystal 1 and crystal 2 [10]. Some experimental values of σ and S_D for a specific $\Delta\theta$ are listed in Table 1 and can be compared with the theoretically predicted values of σ and S_D, calculated from equations (1) and (2), for both Au–Ag and Au–Pd, in Table 2 for $\Delta\theta$ from 0–15° intervals. See also Figs. 5 and 6.

In the Au–Ag case, the lattice parameter difference ($\Delta a/a \sim 0.2\%$) is small. Therefore the interfacial dislocation structure of Au–Ag is similar to that of Au–Au; that is, the character of the interfacial dislocation of Au–Ag is screw dominated (or the edge character is not significant). From the predicted σ values listed in Table 2, it is clear that the edge character of the Au–Ag interfacial dislocations could be detected only for very small $\Delta\theta$, less than about 1°. However, the irregularity of the dislocation network for small $\Delta\theta$ made it impossible to observe any edge character. In fact, the variation in the orientation of various dislocation axes is larger than the predicted σ value in the small $\Delta\theta$ regime. Therefore, the edge character of Au–Ag interfacial dislocations was not successfully confirmed.

For the larger lattice parameter difference $\Delta a/a \sim 4.8\%$ of Au–Pd, the predicted σ value is now large enough to enable us to observe more easily the edge character of twist interphase boundary dislocations. Our experimental results show that the interfacial microstructure of an Au–Pd interface with a small twist angle (<5°) does indeed consist of an orthogonal grid of dislocations, but now the dislocation axis is no longer parallel to the ⟨110⟩ direction,

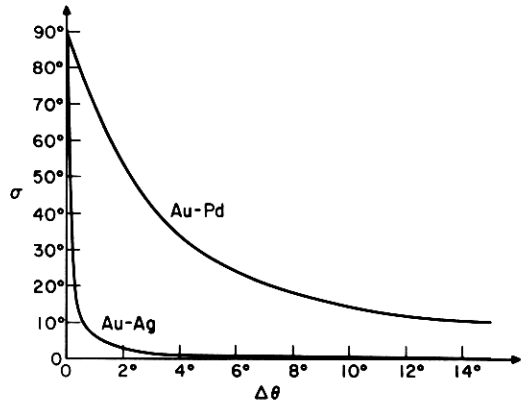

Fig. 5. σ vs $\Delta\theta$ relationship of Au–Ag and Au–Pd bimetallic thin film couples with (001) interfaces predicted by equation (1). The edge character ($\sigma \neq 0$) in Au–Ag system is not significant except for $\Delta\theta < 2°$.

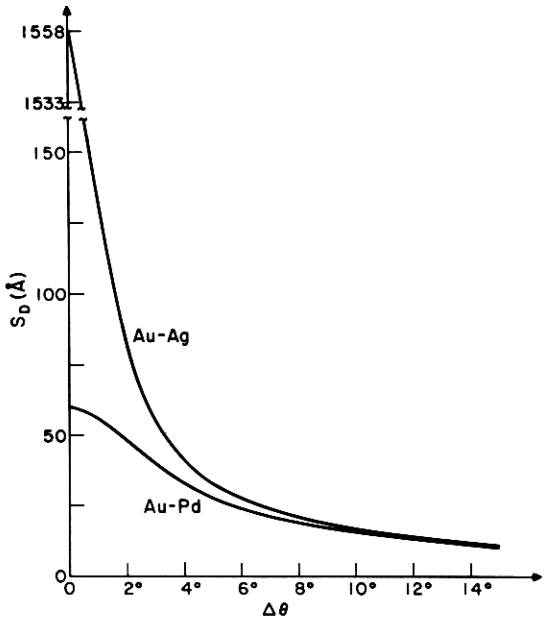

Fig. 6. S_D vs $\Delta\theta$ relationship of Au–Ag and Au–Pd bimetallic thin film couples with (001) interfaces predicted by equation (2). S_D is function of both $\Delta\theta$ and Δa.

as would be expected for a pure screw dislocation in a fcc crystal.

The experimental values of σ and S_D for $\Delta\theta = 2.2°$ and 4.5° are $\sigma \sim 52°$, $S_D \sim 47$ Å and $\sigma \sim 29°$, $S_D \sim 31$ Å, respectively, and the predicted values are $\sigma = 51°$, $S_D = 47$ Å and $\sigma = 31°$, $S_D = 31$ Å, respectively. See Tables 1 and 2. The experimental results thus fit the predicted values quite satisfactorily.

We have thus experimentally demonstrated that the interfacial dislocations of Au–Pd low-angle twist interphase boundaries do indeed show mixed edge-screw character as predicted by the dislocation model for the twist interface proposed by Jesser and Kuhlmann-Wilsdorf [9].

High angle {001} twist interphase boundaries of Au–Ag bicrystals were also investigated. The near coincidence site lattice of $\Sigma = 5$ is expected to occur at the critical angle 36.9°, as predicted for a gold–gold twist grain boundary [5], inasmuch as the lattice parameter difference of gold and silver is so small ($\Delta a/a \sim 0.2\%$). The nature of the high-angle twist grain boundaries in Au–Au have been studied in some

Table 1. The experimental values of S_D and σ in Au–Ag and Au–Pd thin film couples

	Au–Ag		Au–Pd	
$\Delta\theta$(°)	S_D(Å)	σ(°)	S_D(Å)	σ(°)
1.5 ± 0.1	135 ± 14	2 ± 4		
2.2 ± 0.1			47 ± 5	52 ± 4
3.5 ± 0.1	46 ± 5	4 ± 4		
4.0 ± 0.1	42 ± 4	4 ± 4		
4.5 ± 0.1			31 ± 3	29 ± 4

Table 2. The predicted S_D and σ values in equations (1) and (2) for Au–Ag and Au–Pd

$\Delta\theta$(°)	S_D(Å)	σ(°)	S_D(Å)	σ(°)
	(Au–Ag)		(Au–Pd)	
0.0	1558	90.0	60	90.0
0.5	323	12.2	59	79.5
1.0	164	6.2	56	69.7
1.5	110	4.1	52	60.9
2.0	83	3.1	48	53.5
2.5	66	2.5	44	47.2
3.0	55	2.1	40	42.0
3.5	47	1.8	37	37.6
4.0	41	1.5	33	34.0
4.5	37	1.4	31	31.0
5.0	33	1.2	28	28.4
5.5	30	1.1	26	26.1
6.0	28	1.0	25	24.2
6.5	25	1.0	23	22.5
7.0	24	0.9	22	21.1
7.5	22	0.8	20	19.8
8.0	21	0.8	19	18.6
8.5	19	0.7	18	17.6
9.0	18	0.7	17	16.7
9.5	17	0.7	16	15.8
10.0	17	0.6	16	15.1
10.5	16	0.6	15	14.4
11.0	15	0.6	14	13.8
11.5	14	0.5	14	13.2
12.0	14	0.5	13	12.6
12.5	13	0.5	13	12.1
13.0	13	0.5	12	11.7
13.5	12	0.5	12	11.3
14.0	12	0.4	11	10.9
14.5	11	0.4	11	10.5
15.0	11	0.4	11	10.1

In Au–Ag System, $a_1 = a_{Au} = 4.0785$ Å $a_2 = a_{Ag} = 4.0862$ Å.
In Au–Pd System, $a_1 = a_{Pd} = 3.8907$ Å $a_2 = a_{Au} = 4.0785$ Å.

detail by Balluffi *et al.* [5–8]. They have suggested that the Burgers vector of the dislocations at the interface of a twist grain boundary for $\Sigma = 5$ is $\frac{a}{10}\langle 310\rangle$ instead of the $\frac{a}{2}\langle 110\rangle$ primary dislocations found for the low-angle twist grain boundaries. These dislocations are termed 'secondary dislocations.' In this case the $\mathbf{g}\cdot\mathbf{b} = 0$ criterion can be met by $\mathbf{g} = (\bar{3}11)$.

In the Au–Ag specimen of this study, with twist angles near the critical angle 36.9° for $\Sigma = 5$ coincidence, we also found a secondary dislocation network with the dislocation axis parallel to the $\langle 310\rangle$ direction. One set of dislocations is out of contrast when $\mathbf{g} = (1\bar{3}1)$ is operating, as shown in Fig. 7. These results are identical to the case of $\Sigma = 5$ in the high-angle twist grain boundary for Au–Au. The experimental evidence of the secondary dislocation network in the Au–Pd specimen has not yet been obtained, although some critical angles for near coincidence in Au–Pd have been predicted (see Appendix).

In addition to the experimental studies on the identification of the interfacial microstructure, we have also studied the fine structure of the diffraction pattern found in bi-crystal couples. This diffraction pattern is characterized by two simultaneously recorded single crystal diffraction patterns with a relative rotation corresponding to the local twist angle plus reflections due to double diffraction and some other rather weak extra reflections. The origin of these rather weak extra reflections has been suggested to be due to scattering from the two-dimensional periodic array of the interfacial dislocations [7, 11, 12], and not from lattice double diffraction. Figure 8 illustrates that in the system studied the 2-dimensional dislocation grids do indeed give rise to the observed extra spots in the diffraction pattern of the bi-crystal couple. The welding technique that we developed, using no external stress, allows us to examine the microstructure as well as the diffraction pattern on a bi-crystal thin film couple before annealing. The bright-field image under these conditions shows the expected moiré fringe pattern. No interfacial dislocations have yet formed and the accompanying SAD pattern shows a clear double diffraction pattern but no additional weak extra reflections. After annealing, the bright-field image shows interfacial dislocations and the corresponding SAD pattern now does have extra reflections. It is clear that while the double diffraction conditions are the same before and after annealing, the only difference annealing makes is the formation of interfacial dislocations and the accompanying extra reflections are clearly due to the presence of the dislocation grids. Furthermore, their direction and spacing in reciprocal space are what one would expect for the periodic distribution of dislocations observed in real space.

DISCUSSION AND CONCLUSION

The {001} interfacial microstructure of the twist interface of {001} oriented Au–Ag and Au–Pd bi-crystals have been systematically characterized. The interfacial microstructure is characterized by an orthogonal dislocation network. The mixed edge and screw character predicted by W. A. Jesser and D. Kuhlmann-Wilsdorf [9] for the twist interphase boundary dislocations for crystals of differing lattice parameters has been verified for several cases in the present study. In particular, good agreement between experimental and predicted values of σ and S_D has been obtained. The {001} interfacial microstructure of different f.c.c. materials thus retains the expected 4-fold crystallographic symmetry by the generation of an orthogonal dislocation grid. Further, the interphase boundary dislocation adjusts its edge-screw character to efficiently take care of any lattice parameter misfit and misorientation.

The high-angle twist interphase boundary can be understood in terms of the coincidence site lattice concept [13–18] in a like manner to bi-crystals of identical metals, although the rigorously predicted coincidence no longer is expected in the bi-metallic twist interphase boundary. Instead, we describe (see Appendix) a near coincidence approach, where the interphase boundary can reduce its energy by having some

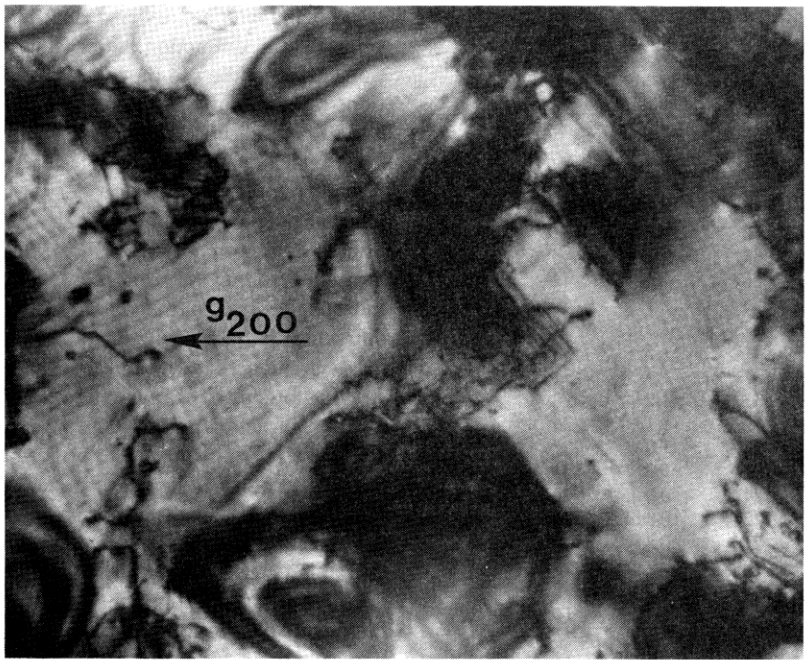

(a)

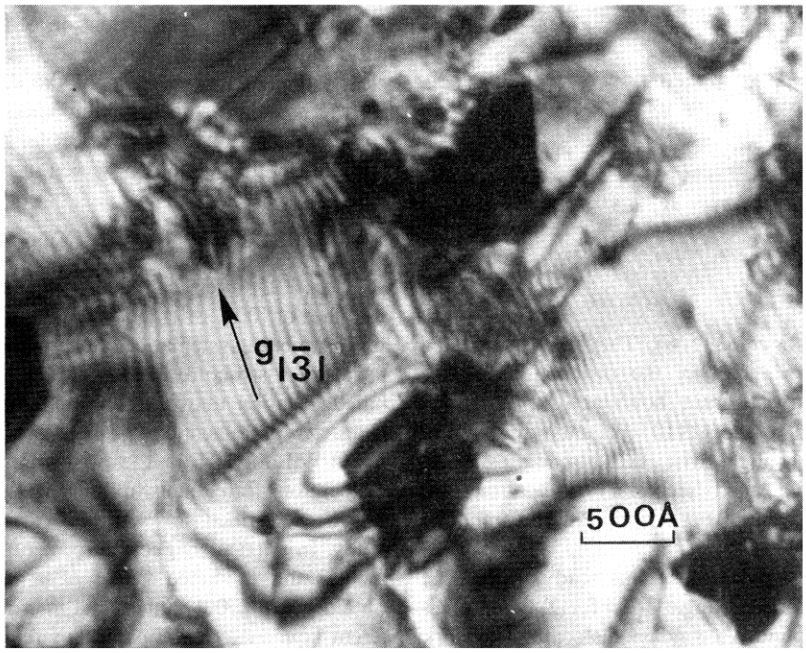

(b)

Fig. 7. The high-angle twist interphase boundary microstructure in Au–Ag near $\theta_c = 36.9°$ for $\Sigma = 5$. (a) A cross grid of secondary dislocation network appears when $\mathbf{g} = (200)$ and zone axis = [001]. (b) One set of the parallel dislocation is out of contrast when $\mathbf{g} = (1\bar{3}1)$ and zone axis = [013].

of the lattice points of both crystals in near-coincidence. There are, in fact, several specific rotational angles, defined by the critical angle θ_c, that can give rise to near coincidences between two crystals. For example, in Au–Pd near coincidence lattices exist at $\theta_c = 45°$ with $\Sigma_{Au} = 8$, $\Sigma_{Pd} = 9$ and at $\theta_c = 18.4°$ with $\Sigma_{Au} = 9$, $\Sigma_{Pd} = 10$ in the {001} interface of Au–Pd (see Appendix for details). The experimental characterization of the high-angle twist interfacial microstructure of Au–Pd is currently under study.

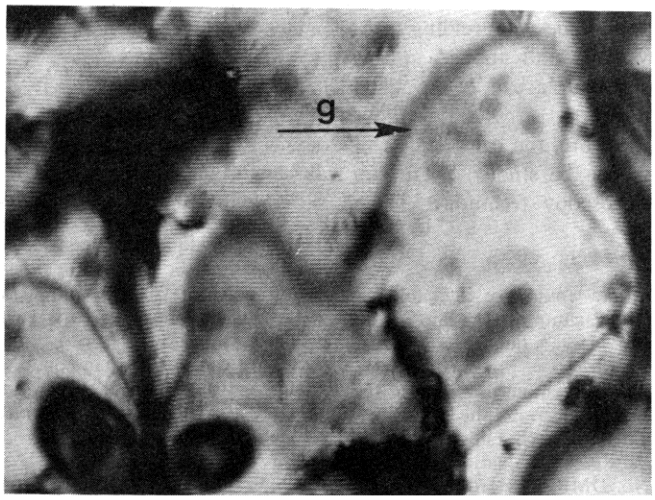

(a)

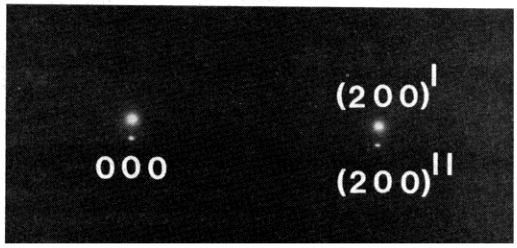

(b)

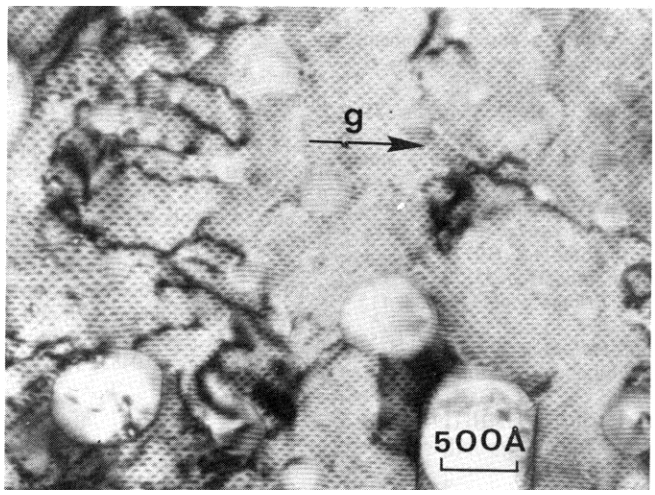

(c)

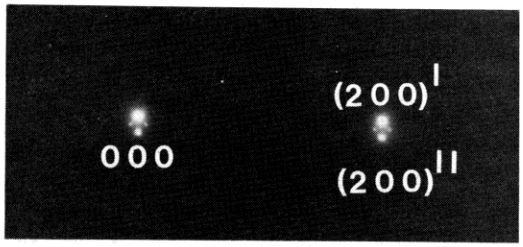

(d)

Fig. 8. Bright-field images and the corresponding SAD pattern of a Au–Ag thin film couple with $\Delta\theta \sim 4°$. (a) Before annealing, the bright-field image shows the moiré fringe pattern. No interfacial dislocations have yet formed. (b) The SAD pattern shows a clear double diffraction pattern but no additional extra reflections. (c) After annealing at 400°C (673 K) in air for 2 min, the bright-field image shows interfacial dislocations. (d) The corresponding SAD pattern now shows extra reflections. These extra reflections are due to diffraction from the dislocation grids.

The significant advantage of the new welding technique that we have developed and applied in this work is that the bi-crystal couple can be obtained without imposition of an external stress and without any further annealing. Therefore, the early stages of the dislocation formation can be studied by *in situ* transmission electron microscopy technique. These studies are also ongoing.

Acknowledgements—The authors would like to thank Dr. F. Cosandey for providing the vacuum system, and for his helpful discussions on improving the quality of metallic thin films.

We also wish to thank the anonymous reviewer of the paper for some helpful remarks concerning the Appendix.

Support from the Materials Research Laboratory Section, Division of Materials Research, National Science Foundation under Grant No. DMR 76-81561 A01 is also gratefully acknowledged.

REFERENCES

1. J. W. Matthews, *Phil. Mag.* **6,** 1347 (1961).
2. J. W. Matthews, *Phil. Mag.* **13,** 1207 (1966).
3. J. W. Matthews and W. A. Jesser, *Acta Metall.* **15,** 595 (1967).
4. T. Schober and R. W. Balluffi, *Phil. Mag.* **20,** 511 (1969).
5. T. Schober and R. W. Balluffi, *Phil. Mag.* **21,** 109 (1970).
6. T. Schober, *Phil. Mag.* **22,** 1063 (1970).
7. R. W. Balluffi, G. R. Woolhouse and Y. Komem, *Nature and Behavior of Grain Boundaries*, (edited by H. Hu), Report of AIME Symp., Detroit (1971).
8. R. W. Balluffi, Y. Komem and T. Schober, *Surf. Sci.* **21,** 68 (1972).
9. W. A. Jesser and D. Kuhlmann-Wilsdorf, *Phys. stat. sol.* **31,** 533 (1967).
10. P. B. Hirsch, A. Howie, R. B. Nicholson, D. W. Pashley and M. J. Whelan, *Electron Microscopy of Thin Crystals*, p. 343. Krieger, Huntington, N.Y. (1977).
11. S. L. Sass and R. W. Balluffi, *Phil. Mag.* **33,** 703 (1976).
12. F. W. Schapinte and T. G. Erlings, *Phil. Mag.* **38,** 115 (1978).
13. R. Bonnet and F. Durand, *Phil. Mag.* **31,** 997 (1975).
14. V. M. Ievlev, A. V. Bugakov and V. A. Ammer, *Phys. stat. sol.* (a) **49,** 413 (1978).
15. W. Bollmann, *Phil. Mag.* **16,** 363(I), 383(II) (1967).
16. W. Bollmann, *Crystal Defects and Crystalline Interfaces*, Springer-Verlag, Berlin, (1970).
17. W. Bollmann, *Surf. Sci.* **31,** 1 (1972).
18. H. Grimmer, W. Bollmann and D. H. Warrington, *Acta Crystallogr.* **197,** A30 (1974).

APPENDIX

A geometrical method can be used to ascertain when coincidence should exist in the dissimilar metal interphase boundaries used in this study. For example, if we consider the {001} twist boundary between two f.c.c. crystals of lattice parameters a_1 and a_2, the {001} planes are square lattices with the lattice parameters $a_1/\sqrt{2}$ and $a_2/\sqrt{2}$. A two-dimensional coincidence site lattice (CSL) will then be produced by rotating these two square lattices about their common ⟨001⟩ axis through an angle θ (see Fig. A-1) such that

$$\frac{a_1^2}{a_2^2} = \frac{m^2 + n^2}{k^2 + l^2}; \tag{A-1}$$

and

$$\theta = \tan^{-1}\left(\frac{n}{m}\right) - \tan^{-1}\left(\frac{l}{k}\right) \tag{A-2}$$

where k, l, m, n are integers without a common factor. Because of the 4-fold symmetry of the square lattice, only angles between 0 and $\pi/4$ need be considered.

Equation (A-1) is the criterion for exact coincidence between two square lattices. However, this condition will rarely, if ever, be satisfied in practice since the right-hand side of equation (A-1) is rational, and the left hand side is invariably irrational in real systems due to the irrational values for all known lattice parameters. However, near coincidence can occur when equation (A-1) is only approximately satisfied if a sufficiently small misfit f exists. This misfit, f, which has been termed 'deformation' [14] is defined by:

$$f = \frac{2|(k^2 + l^2)^{1/2}a_1 - (m^2 + n^2)^{1/2}a_2|}{(k^2 + l^2)^{1/2}a_1 + (m^2 + n^2)^{1/2}a_2}. \tag{A-3}$$

It is always possible to find a solution with arbitrarily small f value by going to large Σ values or with small Σ values by going to large f values. However, such solutions are unlikely to be of practical importance.

Several sets of integers (k, l, m, n) yield the same CSL. Examples are given in Table A-1. The reciprocal coincidence densities of crystal 1 and 2, Σ_1 and Σ_2 are given by

$$\Sigma_1 = k^2 + l^2 \tag{A-4}$$

$$\Sigma_2 = m^2 + n^2 \tag{A-5}$$

when (k, l, m, n) are the set of integers which produce the primitive CSL.

In the Au–Ag system, $a_1 = a_{Au} = 4.0785$ Å, $a_2 = a_{Ag} = 4.0862$ Å and the misfit $\delta(= \Delta a/\bar{a})$ is 0.0019. The lowest order near coincidence site lattices exist at $\theta_c = 36.87°$, 22.62° and 28.07° corresponding to $\Sigma = 5$, 13, 17, etc. See Table A-1. These interphase boundary coincidences are quite similar to the grain boundary coincidences observed in similar metal systems because of the very small difference in the lattice parameters of gold and silver.

A different situation is found for the Au–Pd system, when $a_1 = a_{Au} = 4.0785$ Å, $a_2 = a_{Pd} = 3.8907$ Å and the misfit is thus $\delta = 0.0483$. The two lowest Σ value coinci-

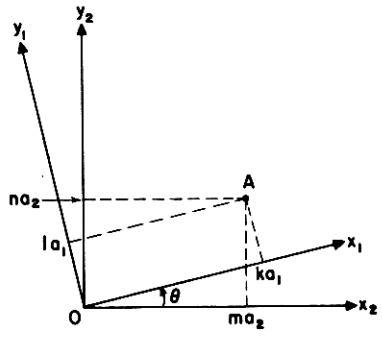

Fig. A-1. The geometry of interphase coincidence boundaries (ICB) between two square lattices rotated with an angle θ. Origin 0 is a common point of both lattices, i.e., a coincident point. Point A is assumed to be a coincident point of the corresponding rotational angle θ.

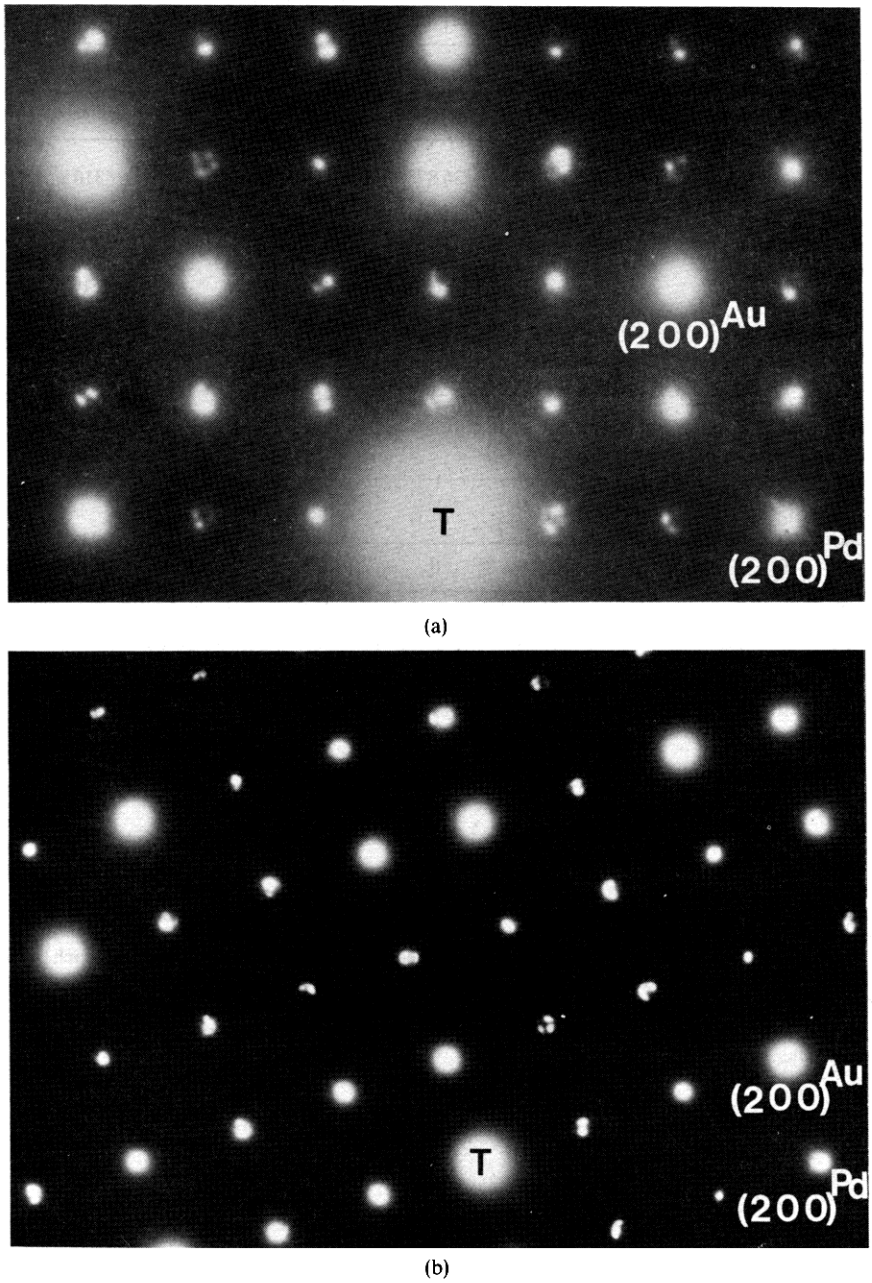

Fig. A-2. Diffraction patterns of Au–Pd bicrystal thin film couples. (a) The twist angle is near 45°, the critical angle for near coincidence of $\Sigma_{Au} = 8$ and $\Sigma_{Pd} = 9$ with $f = 1.2\%$. Note that in the square of $(200)_{Au}$, there are eight lattice points of the small square lattice and in the square of $(200)_{Pd}$, there are nine lattice points of small square lattice. (b) The twist angle is near 18.4°, the critical angle for near coincidence of $\Sigma_{Au} = 9$ and $\Sigma_{Pd} = 10$ with $f = 0.6\%$. There are nine and ten lattice points of small square lattice in the square of $(200)_{Au}$ and $(200)_{Pd}$, respectively.

dences with sufficiently small f values occur when θ are equal to 45° and 18.4°. Examples of likely observable interphase coincidence boundaries (ICB) in Au–Pd are listed in Table A-1. The rules for determining the Burgers vectors of such boundary dislocations have previously been given [15–18] and the Burgers vectors are also included in Table A-1 for both dissimilar metal system couples.

The coincidence character of a boundary is most easily identified from electron diffraction patterns, since reciprocal space retains the same periodicity as does real space. Diffraction results obtained for an Au–Pd bi-crystal with rotation angles $\theta \cong 45°$ and 18.4° do show the expected $\Sigma_{Au} = 8$, $\Sigma_{Pd} = 9$ for $\theta \sim 45°$, and $\Sigma_{Au} = 9$, $\Sigma_{Pd} = 10$ for $\theta \sim 18.4°$, see Fig. A-2. This evidence supports our premise that $\theta_c = 45°$ and 18.4° are angular regimes corresponding to near coincidence in real space. We are currently pursuing studies to image the interfacial dislocation structure of ICB's in Au–Pd.

Table A-1. Selected {001} interphase boundary coincidence relations

(a) Au–Ag†

Σ	k_1	l_1	m_1	n_1	θ_c	f	Burgers vector
5	2	1	2	1	36.87°	0.0019	$\frac{a}{10}\langle 310\rangle$
	3	1	3	1			
	5	0	4	3			
13	3	2	3	2	22.62°	0.0019	$\frac{a}{26}\langle 510\rangle$
	5	1	5	1			
	13	0	12	5			
17	4	1	4	1	28.07°	0.0019	$\frac{a}{34}\langle 530\rangle$
	5	3	5	3			
	17	0	15	8			

(b) Au–Pd‡

Σ_1	Σ_2	k_1	l_1	m_1	n_1	θ_c	f	Burgers vector
8	9	2	2	0	3	45.00°	0.0117	$\frac{a_1}{6}\langle 110\rangle_1 \cong \frac{a_2}{4}\langle 100\rangle_2$
		4	0	3	3			
9	10	3	0	3	1	18.43°	0.0055	$\frac{a_1}{10}\langle 210\rangle_1 \cong \frac{a_2}{6}\langle 110\rangle_2$
		3	3	2	4			
29	32	5	2	4	4	23.20°	0.0021	$\frac{a_1}{8}\langle 100\rangle_1 \cong \frac{a_2}{58}\langle 730\rangle_2$
		3	7	0	8			
41	45	5	4	3	6	24.78°	0.0006	$\frac{a_1}{30}\langle 310\rangle_1 \cong \frac{a_2}{82}\langle 910\rangle_2$
		1	9	$\bar{3}$	9			

† The three lowest Σ-value ICB are given. Three sets of k, l, m, n are given for each ICB. The first set corresponds to the primitive CSL, the second set corresponds to the equivalent centered CSL, and the third set corresponds to a more complex CSL.

‡ The two lowest Σ-value ICB with $f < 0.02$ and the two lowest Σ-value ICB with $f < 0.0025$ are given.